

Development of composite control-variate stratified sampling approach for efficient stochastic calculation of molecular integrals

Michael G. Bayne¹ and Arindam Chakraborty^{1, a)}

Department of Chemistry, Syracuse University, Syracuse, New York 13244 USA

(Dated: 10 November 2021)

Efficient evaluation of molecular integrals is central for quantum chemical calculations. Post Hartree-Fock methods that are based on perturbation theory, configuration interaction, coupled-cluster, and many-body Green's function based methods require access to 2-electron molecular orbital (MO) integrals in their implementations. In conventional methods, the MO integrals are obtained by the transformation of pre-existing atomic orbital (AO) integrals and the computational efficiency of AO-to-MO integral transformation has long been recognized as one of the key computational demanding steps in many-body methods. In this work, the composite control-variate stratified sampling (CCSS) method is presented for calculation of MO integrals without transformation of AO integrals. The central idea of this approach is to obtain the 2-electron MO integrals by direct integration of 2-electron coordinates. This method does not require or use pre-computed AO integrals and the value of the MOs at any point in space is obtained directly from the linear combination of AOs. The integration over the electronic coordinates was performed using stratified sampling Monte Carlo method. This approach was implemented by dividing the integration region into a set of non-overlapping segments and performing Monte Carlo calculations on each segment. The Monte Carlo sampling points for each segment were optimized to minimize the total variance of the sample mean. Additional variance reduction of the overall calculations was achieved by introducing control-variate in the stratified sampling scheme. The composite aspect of the CCSS allows for simultaneous computation of multiple MO integrals during the stratified sampling evaluation. The main advantage of the CCSS method is that unlike rejection sampling Monte Carlo methods such as Metropolis algorithm, the stratified sampling uses all instances of the calculated functions for the evaluation of the sample mean. The CCSS method is designed to be used for large systems where AO-to-MO transformation is computationally prohibitive. Because it is based on numerical integration, the CCSS method can be applied to a wide variety of integration kernels and does not require *a priori* knowledge of analytical integrals. In this work, the developed CCSS method was applied for calculation of exciton binding energies in CdSe quantum dots using electron-hole explicitly correlated Hartree-Fock (eh-XCHF) method and excitation energy calculations using geminal-screened electron-hole interaction kernel (GSIK) method. The results from these calculations demonstrate that the CCSS method enabled the investigation of excited state properties of quantum dots by avoiding the computationally challenging AO-to-MO integral transformation step.

Keywords: Monte Carlo

I. INTRODUCTION

Matrix elements of molecular orbitals (MOs) are central to quantum chemical calculations. The MOs form a natural choice for single-particle basis functions used in the second-quantized representation for many-body post Hartree-Fock (HF) theories. In the LCAO-MO represen-

tation, each molecular orbital is represented as a linear combination of a set of atomic orbitals. The expansion coefficients of the MOs in terms of the AOs are obtained by solving the pseudo-eigenvalue Fock equation using the SCF procedure. Evaluation of the matrix elements in the MO representation requires transformation of the AO integrals. For example, in the case of the two-electron Coulomb integral this expansion is given as,

$$[\psi_p(1)\psi_q(1)|r_{12}^{-1}|\psi_r(2)\psi_s(2)] = \sum_{\mu\nu\lambda\sigma} C_{\mu p}C_{\nu q}C_{\lambda r}C_{\sigma s}[\phi_\mu(1)\phi_\nu(1)|r_{12}^{-1}\omega(1,2)|\phi_\lambda(2)\phi_\sigma(2)]. \quad (1)$$

As seen from Equation 1, the transformation formally

^{a)}corresponding author: archakra@syr.edu

scales as the 4th power of the number of AO basis functions (N_b). There are various situations where efficient computation of MO integrals is required to perform electronic structure calculations. For example, application of many-body theories such as configuration interaction (CI),^{1,2} many-body perturbation theory (MBPT),^{3,4} and couple-cluster theory (CC)⁵ for large chemical systems need fast and efficient access to these MO integrals.

Efficient calculation on MO integrals is a recurrent theme in increasing the efficiency of the electronic structure calculations. The transformation can be accelerated by performing it in parallel and various parallelization algorithms have been developed.⁶⁻⁸ The computational cost can also be reduced using rank-reduction techniques such as resolution-of-identity⁹⁻¹⁸ and Cholesky decomposition.¹⁹⁻²³ In a series of papers, Martinez *et al.* have developed the tensor-hypercontraction approach²⁴⁻³⁶ that has enabled significant reduction in the computational cost of electron-repulsion integrals (ERI). A current review of the various ERI techniques has been presented by Peng and Kowalski.⁵

Efficient evaluations of MO integrals are also required in explicitly correlated methods³⁷⁻⁴⁴ where the evaluation of the r12-kernel in AO representation is not readily available or is not computationally efficient. For a n-body operator, the AO-to-MO transformation scales as N_b^{2n} and becomes computationally expensive for n-body operators when $n > 2$ because of steep scaling with respect to the number of AO basis functions. This has found to be especially true for explicitly correlated methods for treating electron-electron,^{37,45-51} electron-proton,⁵²⁻⁶⁴ and electron-hole⁶⁵⁻⁷⁵ many-body theories. One approach to avoid the transformation of the AO integrals is to use real-space representation and to evaluate the MO integrals numerically. This procedure requires evaluation of the MOs at any position in the 3D space which can be evaluated from the AO expansion,

$$\psi_p(\mathbf{r}) = \sum_{\mu} C_{\mu p} \phi_{\mu}(\mathbf{r}). \quad (2)$$

This strategy has been used very successfully in quantum Monte Carlo methods⁷⁶⁻⁸³ where evaluation of individual MO integrals can be completely avoided and the entire many-electron integral is evaluated directly in real-space representation using Markov chain Monte Carlo (MCMC) implementation. The MCMC implementation was also shown to be used in the context of perturbation theory in a series of articles by Hirata *et al.*⁴⁷⁻⁵¹ in which MCMC techniques were used for the evaluation of MP2-F12 energies.

In this work we present the composite control-variate stratified sampling (CCSS) Monte Carlo method for efficient calculation of MO integrals. The accuracy of stochastic evaluation of integrals can be systematically improved by reducing the variance of the calculation. In the CCSS method, we have combined both control-variate and stratified sampling strategies for variance reduction. The CCSS method was used in conjunction

with the electron-hole explicitly correlated Hartree-Fock method (eh-XCHF) for the calculation of exciton binding energies and excitation energies in CdSe clusters and quantum dots.

II. THEORY

A. Coordinate transformations

We start by defining the following general two-electron integral of the following form,

$$I_{pqrs} = \iint_{-\infty}^{+\infty} d\mathbf{r}_1 d\mathbf{r}_2 \Lambda_{pq}(1) \Lambda_{rs}(2) r_{12}^{-1} \omega(1, 2), \quad (3)$$

where $\Lambda_{pq} = \psi_p \psi_q$ and $\Lambda_{rs} = \psi_r \psi_s$. We will transform the two-electron coordinate system into intracuclear and extracuclear coordinates,

$$\mathbf{r}_{12} = \mathbf{r}_1 - \mathbf{r}_2 \quad (4)$$

$$\mathbf{R} = \frac{1}{2}(\mathbf{r}_1 + \mathbf{r}_2). \quad (5)$$

The Jacobian for this transformation is,

$$d\mathbf{r}_1 d\mathbf{r}_2 = d\mathbf{R} d\mathbf{r}_{12}. \quad (6)$$

In the next step, we will transform into spherical polar coordinates,

$$d\mathbf{r}_{12} = r_{12}^2 \sin(\theta_{12}) dr_{12} d\theta_{12} d\phi_{12} \quad (7)$$

$$d\mathbf{R} = R^2 \sin(\Theta) dR d\Theta d\Phi. \quad (8)$$

Using Equation 7, the integral Equation 3 is,

$$I_{pqrs} = \int_0^{\infty} dR dr_{12} r_{12} R^2 \int_0^{\pi} d\Theta d\theta_{12} \sin^2 \Theta \sin^2 \theta_{12} \int_0^{2\pi} d\Phi d\phi \Lambda_{pq}(1) \Lambda_{rs}(2) \omega(1, 2). \quad (9)$$

The transformation to the spherical polar coordinates allows us to analytically remove the r_{12}^{-1} singularity in the integration kernel. In many applications, the operator $\omega(1, 2)$ might depend only on r_{12} in which case it can be moved out of the integration over the angular coordinates. For performing Monte Carlo calculation to evaluate this integral numerically, it is convenient to transform the integration limits to $[0, 1]$. Now we will perform a third coordinate transformation and transform the integration domain to $[0, 1]$ limits. This is done mainly to aid in the numerical evaluation of the integral using Monte Carlo techniques. We define a new set of coordinates ($\mathbf{t} = \{t_1, t_2, \dots, t_6\}$) where each coordinate is in

the range $t \in [0, 1]$. The radial and angular coordinates are transformed as,

$$r = \frac{t}{1-t} \quad (10)$$

$$\theta = \frac{t}{\pi} \quad (11)$$

$$\phi = \frac{t}{2\pi}. \quad (12)$$

The associated Jacobians are,

$$dr = \frac{1}{(1-t)^2} dt \quad (13)$$

$$d\theta = \frac{1}{\pi} dt \quad (14)$$

$$d\phi = \frac{1}{2\pi} dt. \quad (15)$$

In the t -space, the expression for I_{pqrs} can be expressed compactly as,

$$I_{pqrs} = \int_0^1 dt f(\mathbf{t}). \quad (16)$$

The integral kernel $f(\mathbf{t})$ is obtained by substituting Equation 10 and Equation 13 into Equation 9,

$$f(\mathbf{t}) = \left(\frac{1}{2\pi^2} \right)^2 \frac{t_1}{(1-t_1)^3} \frac{t_2^2}{(1-t_2)^4} \sin(t_3/\pi) \sin(t_4/\pi) \Lambda_{pq}(\mathbf{t}) \omega(\mathbf{t}) \Lambda_{rs}(\mathbf{t}), \quad (17)$$

where t_1 and t_2 corresponds to r_{12} and R , respectively, and the remaining t_i are angular coordinates. Using Monte Carlo, the estimation of I_{pqrs} is then given by the following expression,

$$I_{pqrs} \approx \mathbb{E}[f] \pm \sqrt{\frac{\mathbb{V}[f]}{N_S}}, \quad (18)$$

where N_S is the number of sampling points and \mathbb{E} is the expectation value. \mathbb{V} is the variance defined by Equation 19 and Equation 20, respectively, and is shown below,

$$\mathbb{E}[f] = \frac{1}{N_S} \sum_{i=1}^{N_S} f(\mathbf{t}_i) \quad (19)$$

$$\mathbb{V}[f] = \mathbb{E}[f^2] - \mathbb{E}[f]^2. \quad (20)$$

A summary of key relationships between expectation value and variance that is relevant to this derivation is provided in appendix A. As seen from Equation 18, the error in the numerical estimation of the integral depends on the variance, hence it is desirable to reduce the overall variance of the sampling to obtain an accurate value of the integral. In this work, we have combined stratified sampling approach with the control-variate method to achieve variance reduction.

B. Stratified sampling

Stratified sampling is a successful strategy to reduce the variance of the overall estimate of the calculation.

This is a well-know technique that has been described earlier in previous publications.^{84–88} Here, only the key features of the method that are directly related to this work are summarized below. Stratified sampling can be implemented using both constant-volume or different-volume segments, and in this work we have used only the constant volume version. In the constant-volume approach, the integration domain Ω of the integration region is uniformly divided among non-overlapping segments (Equation 21),

$$\Omega = \sum_{\alpha=1}^{N_{\text{seg}}} \Omega_{\alpha}. \quad (21)$$

We have used a direct-product approach for generation of the segments. Along each t -dimension, the region $[0, 1]$ was divided equally into 2^m segments. The segments for the 6-dimension was obtained by the direct-products of the 1-dimensional segments. This procedure resulted in a total of $N_{\text{seg}} = 2^{6m}$ number of 6D segments. The sample mean and variance associated with each segment α is given as,

$$\mu_{\alpha} = \mathbb{E}[f_{\alpha}] = \frac{1}{N_S^{\alpha}} \sum_{\mathbf{t} \in \Omega_{\alpha}} f(\mathbf{t}), \quad (22)$$

where N_S^{α} is the number of sampling points used in the evaluation of the expectation value for segment α . The notation $\mathbf{t} \in \Omega_{\alpha}$ implies that points only in the domain Ω_{α} should be used for evaluation of the expectation value \mathbb{E} . Analogous to Equation 20, the variance associated with each segment is defined as,

$$\sigma_{\alpha}^2 = \mathbb{V}[f_{\alpha}] = \mathbb{E}[f_{\alpha}^2] - \mathbb{E}[f_{\alpha}]^2. \quad (23)$$

The estimate of the total expectation value is obtained by the average over all the segments. Mathematically, this can be expressed as,

$$\mathbb{E}[f] = \mu = \frac{1}{N_{\text{seg}}} \sum_{\alpha=1}^{N_{\text{seg}}} \mu_{\alpha}. \quad (24)$$

In [Equation 24](#), partial averages from all the segments contribute equally because all the segments have exactly identical volumes. For cases where segments have different volumes, the above expression should be replaced by a weighted average. To calculate the variance on μ we will use the relationship that the variance of sum of two random variates are related to each other by their covariance (derived in [Equation A17](#)) as shown below,

$$\mathbb{V}[\sum_i a_i X_i] = \sum_{ij} a_i a_j \mathbb{C}[X_i, X_j], \quad (25)$$

where covariance \mathbb{C} defined as,

$$\mathbb{C}[X, Y] = \mathbb{E}[XY] - \mathbb{E}[X]\mathbb{E}[Y]. \quad (26)$$

Using the relationship in [Equation 26](#),

$$\mathbb{V}[\mu] = \mathbb{V}\left[\frac{1}{N_{\text{seg}}} \sum_{\alpha=1}^{N_{\text{seg}}} \mu_{\alpha}\right] \quad (27)$$

$$= \frac{1}{N_{\text{seg}}^2} \sum_{\alpha\beta} \mathbb{C}[\mu_{\alpha}, \mu_{\beta}]. \quad (28)$$

Because the sampling of any two segments are completely uncorrelated, all the off-diagonal elements of the covariance matrix will be zero,

$$\mathbb{C}[\mu_{\alpha}, \mu_{\beta}] = \mathbb{V}[\mu_{\alpha}] \delta_{\alpha\beta}. \quad (29)$$

Using [Equation 29](#) and result from [Equation A21](#),

$$\mathbb{V}[\mu] = \frac{1}{N_{\text{seg}}^2} \sum_{\alpha} \mathbb{V}[\mu_{\alpha}]. \quad (30)$$

The result from [Equation 30](#) implies that the variance of the mean always decreases with increasing number of segments. The variance of the segment mean, μ_{α} , is related to related to sample variance by the following relationship (derived in [Equation A24](#)),⁸⁴⁻⁸⁸

$$\mathbb{V}[\mu_{\alpha}] = \frac{\mathbb{V}[f_{\alpha}]}{N_S^{\alpha}}. \quad (31)$$

This implies,

$$\mathbb{V}[\mu] = \frac{1}{N_{\text{seg}}^2} \sum_{\alpha} \frac{\mathbb{V}[f_{\alpha}]}{N_S^{\alpha}}. \quad (32)$$

The central idea of stratified sampling is to optimize the distribution of sampling points across all segments to reduce the variance in the mean. To achieve this, a normalized weight factor, w_{α} , is associated with each segment and is given by,

$$\sum_{\alpha}^{N_{\text{seg}}} w_{\alpha} = 1 \quad \text{and} \quad w_{\alpha} \geq 0. \quad (33)$$

The number of sampling points for each segment is given by a fraction of the total number of sampling points,

$$N_S^{\alpha} = w_{\alpha} N_T. \quad (34)$$

Substituting in [Equation 32](#),

$$\mathbb{V}[\mu] = \frac{1}{N_{\text{seg}}^2 N_T} \sum_{\alpha} \frac{1}{w_{\alpha}} \mathbb{V}[f_{\alpha}]. \quad (35)$$

It can be shown that the optimal distribution of points is achieved by selecting the weights proportional to the standard-deviations of each segment,⁸⁴⁻⁸⁸

$$\min_{\mathbf{w}} \mathbb{V}[\mu] \rightarrow w_{\alpha}^{\text{opt}} = \frac{\sqrt{\mathbb{V}[f_{\alpha}]}}{\sum_{\beta}^{N_{\text{seg}}} \sqrt{\mathbb{V}[f_{\beta}]}}. \quad (36)$$

The above equation very nicely illustrates the intuitive logic behind stratified sampling that segments with higher variance (or standard deviation) should receive proportionally more sampling points than regions with lower variance. The optimized distribution of weights and inverse dependence on the number of segments are the two main reasons why stratified sampling is an effective technique for variance reduction.

C. Variance reducing using control-variate

Control-variate is another strategy that has been used in past for reducing the variance of Monte Carlo calculations.⁸⁴⁻⁸⁸ In this work, we have incorporated control-variate technique in our stratified sampling calculations. In control-variate methods, we start with a function (denoted as $f_0(\mathbf{t})$) whose integral is known in advance,

$$I_{pqrs}^0 = \int_0^1 dt f_0(\mathbf{t}). \quad (37)$$

We then add and subtract this quantity from the integral to be evaluated,

$$I_{pqrs} = \int_0^1 dt f(\mathbf{t}) + \eta \left[I_{pqrs}^0 - \int_0^1 dt f_0(\mathbf{t}) \right], \quad (38)$$

where η is a yet to be determined scaling parameter. Rearranging we get,

$$I_{pqrs} = \eta I_{pqrs}^0 + \int_0^1 dt [f(\mathbf{t}) - \eta f_0(\mathbf{t})]. \quad (39)$$

The optimum value of the scaling parameter η is obtained by minimizing the variance given in Equation 35,

$$\min_{\eta} \mathbb{V}[\mu] \rightarrow \eta_{\text{opt}}. \quad (40)$$

Because of the above minimization, the variance obtained from control-variate sampling is always lower or equal to the variance obtained without using control-variate,

$$(\mathbb{V}[\mu])_{\eta_{\text{opt}}} \leq (\mathbb{V}[\mu])_{\eta=0}. \quad (41)$$

Conceptually, control-variate method allows us to perform Monte Carlo calculation only on the component of the f that is different from f_0 . For integration over molecular integrals, one of the simplest control-variate function is the overlap integral,

$$f_0(1, 2) = [\chi_p(1)\chi_q(1)][\chi_r(2)\chi_s(2)] \quad (42)$$

$$I_{pqrs}^0 = \delta_{pq}\delta_{rs}. \quad (43)$$

In the case that the underlying AO integrals are available, a better estimate of f_0 can be constructed. For example, collecting only the diagonal elements of the $\sum_{\mu\nu\lambda\sigma}$ in Equation 1, the control-variate function f_0 can be defined as,

$$f_0(1, 2) = \sum_{\mu}^{N_b} C_{\mu p} C_{\mu q} C_{\mu r} C_{\mu s} \phi_{\mu}(1) \phi_{\mu}(1) r_{12}^{-1} \phi_{\mu}(2) \phi_{\mu}(2). \quad (44)$$

The value of the integral I_0 is obtained analytically from the underlying AO integrals,

$$I_{pqrs}^0 = \sum_{\mu}^{N_b} C_{\mu p} C_{\mu q} C_{\mu r} C_{\mu s} [\phi_{\mu}(1) \phi_{\mu}(1) |r_{12}^{-1}| \phi_{\mu}(2) \phi_{\mu}(2)]. \quad (45)$$

We note that unlike I_{pqrs} , evaluation of I_{pqrs}^0 is linear in terms of number of AO basis function N_b .

D. Composite control-variate stratified sampling

In most applications, matrix elements of a set of molecular orbitals are needed for performing electronic structure calculations. Although in principle the control-variate stratified sampling method presented above can be applied for evaluation of each matrix element, however, such an approach is computationally inefficient. A

more efficient approach is to evaluate the integrals simultaneously for all the matrix elements. We call this approach the composite control-variate stratified sampling (CCSS) and is described as follows.

We start with set of MO indices for which the integrals are needed to be evaluated,

$$\mathcal{Z} = \{(p_1 q_1 r_1 s_1), (p_2 q_2 r_2 s_2), \dots\}. \quad (46)$$

If all the MO integrals are needed, this set will be a set of all symmetry unique indices. All index combination from \mathcal{Z} which are known to be zero because of symmetry arguments are also eliminated from the set. We will use the collective index K to enumerate the individual elements of set \mathcal{Z} ,

$$\mathcal{Z} = \{z_K\}. \quad (47)$$

Because the domain of the integration is identical for all the indices, all the integrals can be evaluated simultaneously,

$$I_K = \eta^K I_K^0 + \int_0^1 dt [f^K(\mathbf{t}) - \eta^K f_0^K(\mathbf{t})]. \quad (48)$$

In terms of segments,

$$I_K = \eta^K I_K^0 + \frac{1}{N_{\text{seg}}} \sum_{\alpha}^{N_{\text{seg}}} \mathbb{E} [f^K - \eta^K f_0^K]. \quad (49)$$

The expectation value for each segment will be evaluated using N_{seg}^{α} number of sample points whose distribution is defined using the weights obtained in Equation 36. However, because each segment is now associated with N_K number of functions, there are w^K weights associated with each segment. In the CCSS method, we renormalize the weights by choosing the maximum weight associated with all the functions for a given segment. Mathematically, this is described by the following equations,

$$x_{\alpha}^{\text{opt}} = \max_K \{w_{\alpha, K}^{\text{opt}}\} \quad (50)$$

$$w_{\alpha}^{\text{opt}} = \frac{x_{\alpha}^{\text{opt}}}{\sum_{\beta} x_{\beta}^{\text{opt}}}. \quad (51)$$

E. Precomputation, run-time computation, and parallelization

In the CCSS method, because the same set of molecular orbitals will be used for calculations of all the integrals in set \mathcal{Z} , it is computationally efficient to compute them once and use them for all functional evaluations. In a single Monte Carlo step in a given segment, first a random vector $\mathbf{t} \in \Omega_{\alpha}$ is obtained and all the MOs at \mathbf{t} are evaluated and stored in a vector \mathbf{v} of size N_{MO} . The functions f^K and f_0^K are then built by reading values from vector \mathbf{v} . These simple steps result in significant savings in

computation time because it avoids repeated evaluations of MO values at point \mathbf{t} for each function evaluation in set \mathcal{Z} .

The implementation of the CCSS method requires the determination of two run-time parameters η^K and w_α^{opt} defined in Equation 40 and Equation 50, respectively. Instead of evaluating them for the entire run, these parameters were determined using data from the first 10% of the run and were kept fixed for the remaining 90% of the calculation. As seen from Equation 50, the evaluation of the weights for each segment requires information from all the segments. By making these weights constant for the 90% of the run time allows for efficient parallelization of the CCSS method by completely decoupling information exchange among the segments. Consequently, this enables Monte Carlo steps for each segment to be performed in parallel. This strategy was found to significantly reduce the computational time of the overall calculation.

III. RESULTS

A. Electron-hole interaction in CdSe quantum dots with dielectric screening

The CCSS method was used for calculating the exciton binding energies in a series of CdSe quantum dots using the electron-hole explicitly-correlated Hartree-Fock (eh-XCHF) method. The eh-XCHF method has been successfully used before⁶⁶ for investigation of excitonic interactions in QDs and only a brief summary relevant to the CCSS method is presented here. In the eh-XCHF method, the electronic excitation in the QD is described using the quasiparticle representation. The electron-hole integration is represented using the following effective quasiparticle Hamiltonian,

$$\hat{H}_{\text{eh}} = \sum_{ij} \langle i | \frac{-\hbar^2}{2m_e} \nabla^2 + v_{\text{ext}}^e | j \rangle e_i^\dagger e_j \quad (52)$$

$$+ \sum_{ij} \langle i | \frac{-\hbar^2}{2m_h} \nabla^2 + v_{\text{ext}}^h | j \rangle h_i^\dagger h_j \quad (53)$$

$$+ \sum_{ij i' j'} K_{ij i' j'}^{\text{eh}} e_i^\dagger e_j h_{i'}^\dagger h_{j'} \quad (54)$$

$$+ \sum_{ijkl} w_{ijkl}^{\text{ee}} e_i^\dagger e_j^\dagger e_l e_k + \sum_{ijkl} w_{ijkl}^{\text{hh}} h_i^\dagger h_j^\dagger h_l h_k, \quad (55)$$

where the unprimed and primed indices represent quasi-electron and quasihole states, respectively. The attractive electron-hole interaction, K^{eh} , is the principle component that results in exciton binding and in these calculations, K^{eh} was approximated using static dielectric screening developed by Wang and Zunger for CdSe QDs.⁸⁹ The electron-hole wave function was represented using the eh-XCHF ansatz which is defined as,

$$\Psi_{\text{eh-XCHF}} = \hat{G} \Phi^e \Phi^h, \quad (56)$$

where,

$$\hat{G} = \sum_{i=1}^{N_e} \sum_{j=1}^{N_h} g(i, j), \quad (57)$$

and g is a linear combination of Gaussian-type geminal functions,

$$g(1, 2) = \sum_{k=1}^{N_g} b_k e^{-\gamma_k r_{12}^2}. \quad (58)$$

In the eh-XCHF method the function g is obtained by the following minimization procedure,

$$E = \min_g \frac{\langle \Phi^e \Phi^h | \hat{G}^\dagger \hat{H}_{\text{eh}} \hat{G} | \Phi^e \Phi^h \rangle}{\langle \Phi^e \Phi^h | \hat{G}^\dagger \hat{G} | \Phi^e \Phi^h \rangle}. \quad (59)$$

The exciton binding energy is calculated as the difference between the interaction and non-interacting energies,

$$E_{\text{EB}} = \langle E_{\text{non-interacting}} \rangle - \langle E_{\text{exciton}} \rangle. \quad (60)$$

The eh-XCHF formulation requires matrix elements of molecular orbitals involving the Coulomb operator r_{12}^{-1} and the Gaussian-type geminal function g and is an ideal candidate to test the CCSS method. In the previous applications of the eh-XCHF method,⁶⁶ these integrals were evaluated using analytical geminal integrals. For testing the CCSS implementation, we calculated the exciton binding energies in CdSe clusters and compared with the previously reported⁶⁶ exciton binding energies obtained using analytical AO integrals. The results from the CCSS methods are summarized in Figure 1. The results show that the exciton binding energies obtained using the CCSS method are in good agreement with the analytical results. We also find that the CCSS are in good agreement with the previously reported exciton binding energies from experimental and theoretical investigations (Figure 2).

B. Excitation energy of CdSe clusters using dynamic screening

The developed CCSS method was applied for the calculation of excitation energy in small CdSe clusters. The electronic excitation was described using electron-hole quasiparticle representation and the electron-electron correlation effect was incorporated using screened electron-hole interaction kernel. In this work, we have used the geminal screened electron-hole interaction kernel which has the following form,

$$K_{\text{eh}}(1, 2) = w(1, 2)g(1, 2)(1 - P_{12}), \quad (61)$$

where $w(1, 2)$ is residual electron-electron interaction operator, $g(1, 2)$ is explicitly-correlated Gaussian-type geminal operator, and the P_{12} is the permutation operator

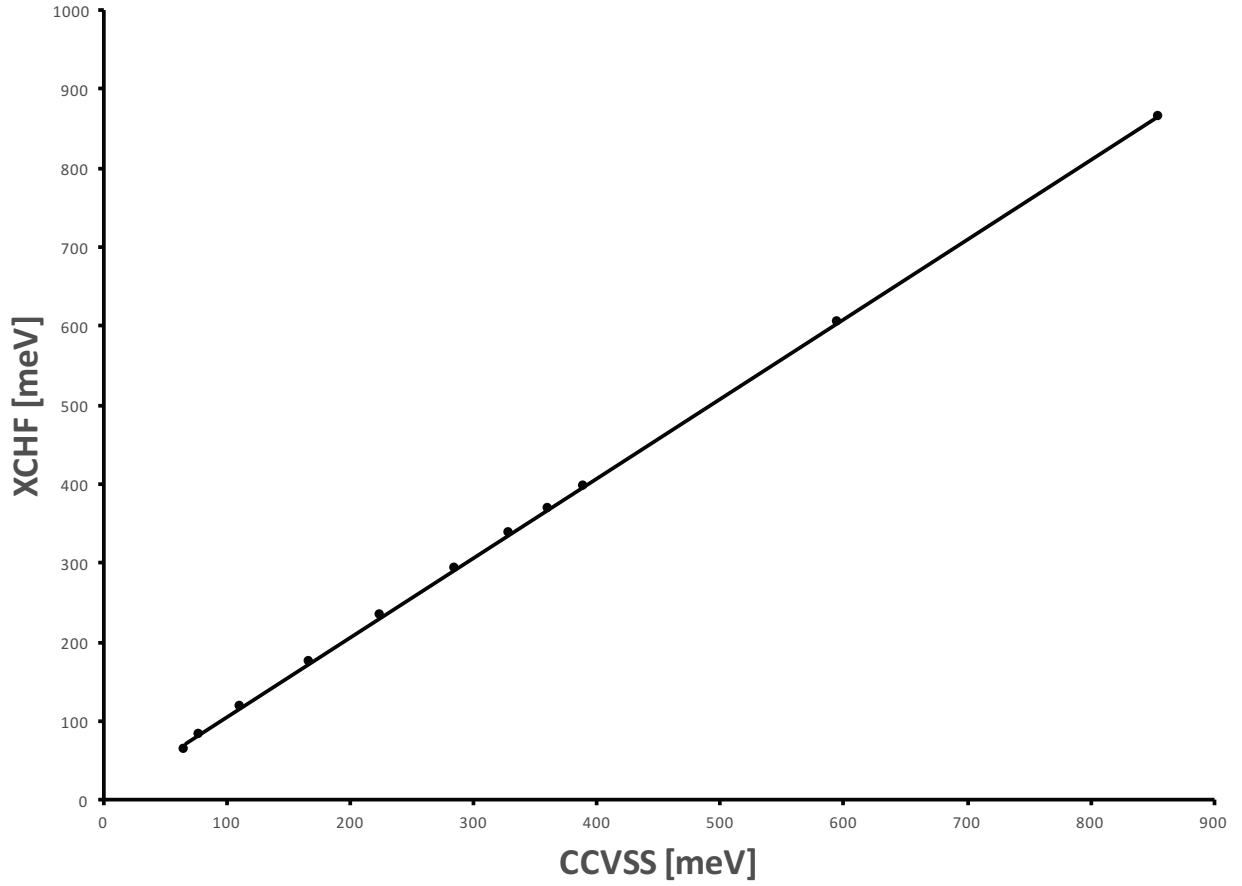


FIG. 1. Binding energies in meV of CdSe quantum dots ranging in size from 1 nm to 20 nm in diameter of the XCHF method on the y-axis and this work on the x-axis. The trendline in this graph has a slope of 1.0072.

TABLE I. Exciton binding energies [meV] for CdSe quantum dots ranging in diameters from 1.24nm to 20nm in size. The standard deviation σ is reported in the last column.

CdSe QD Diameter [nm]	CCSS Binding Energy [meV]	σ [meV]
1.24	855	1.24E-03
1.79	596	2.89E-03
2.76	388	8.24E-03
2.98	360	9.66E-03
3.28	327	1.22E-02
3.79	284	1.68E-02
4.80	225	3.19E-02
6.60	166	7.69E-02
10.0	110	2.72E-02
15.0	75.2	1.02E-02
20.0	57.4	2.64E-02

(Equation 62-Equation 63),

$$\sum_{i<j} r_{ij}^{-1} - \sum_i v_{\text{HF}}(i) = \sum_{i<j} w(i,j) \quad (62)$$

$$P_{12}f(1,2) = f(2,1). \quad (63)$$

Using diagrammatic perturbation theory, it can be shown that up to first-order in g , the excitation energy is given by the following expression,⁷¹

$$\omega = \omega_0 + \langle ia | K_{\text{eh}} | ai \rangle, \quad (64)$$

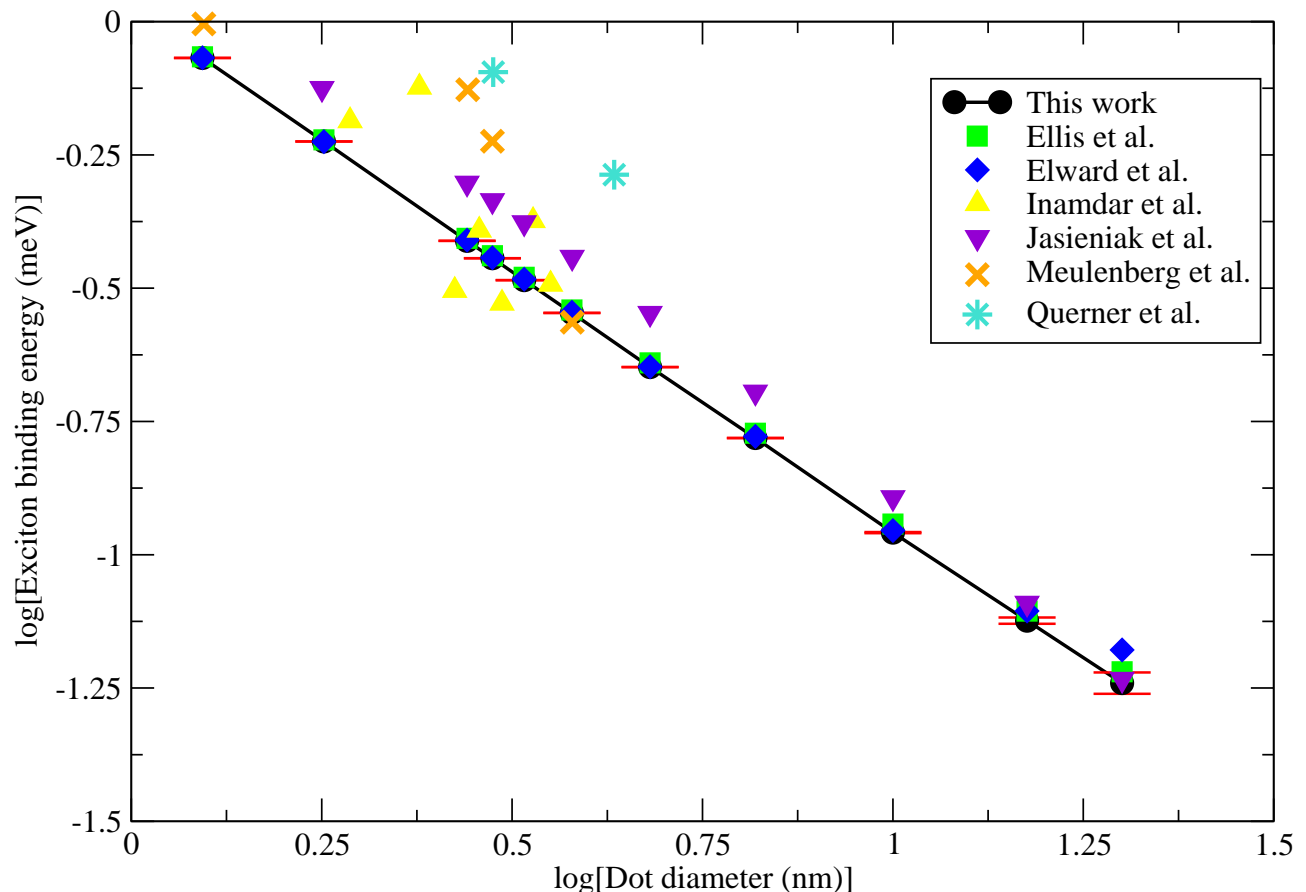


FIG. 2. Binding energies in meV of CdSe quantum dots ranging in size from 1 nm to 20 nm in diameter of this work compared with Ellis et al.,⁹⁰ Elward et al.,⁶⁶ Inamdar et al.,⁹¹ Jasieniak et al.,⁹² Muelenberg et al.,⁹³ and Querner et al.⁹⁴ For the CCSS method, red error bars are shown for the exciton binding energy calculations.

where ω_0 is the independent quasiparticle excitation energy and is equal to the energy difference between the quasihole and quasielectron states ($\omega_0 = \epsilon_a - \epsilon_i$). The evaluation of the matrix element of K_{eh} was accomplished using the developed CCSS method. The single-particle states were obtained from Hartree-Fock calculations using LANL2DZ ECP basis. The Gaussian-type geminal function was expanded using three-term expansions and the expansion coefficients were obtained from literature. The b and γ used in this work were 0.867863 and 0.010425, respectively, for the binding energy calculation on the Cd₂₀Se₁₉ quantum dot. Excitation energy in the Cd₂₀Se₁₉ cluster using the CCSS method was calculated and was found to be $3.14 \pm 4 \times 10^{-4}$ eV. This result was found to be in good agreement with the previously published excitation energy of 3.10 eV obtained using pseudopotential+CI calculation. The application of the geminal-screened electron-hole interaction kernel method using analytical geminal AO integrals were computationally prohibitive for this system, however the developed CCSS method allowed us to overcome the computational barrier (948 basis functions) and apply the explicitly-correlated formulation to the calculation of ex-

citation energy for this system.

IV. CONCLUSION

In conclusion, the development and implementation of the CCSS Monte Carlo method was presented. The CCSS method is a numerical integration scheme that uses Monte Carlo approach for calculation of MO integrals. The accuracy of Monte Carlo evaluation of integrals can be systematically improved by reducing the variance of the sample mean. In the CCSS method, we have combined both control-variate and stratified sampling strategies for variance reduction. The main feature of the CCSS method is that it avoids explicit AO-to-MO integral transformation for evaluation of the MO integrals. Consequently, it only requires value of the spatial MO at a given point which is readily obtained from the linear combination of the AOs. The use of stratified sampling in CCSS method is an important feature because the distribution of sampling points for each segment is optimized to minimize the overall variance. Computa-

tionally, this results in segments with higher variance are sampled proportionally more than segments with lower variance. Another feature of stratified sampling is that all instances of the calculated function are used for the estimation of the integral. This should be contrasted with rejection sampling Monte Carlo methods, where not all function evaluations contribute towards the estimation of the integral. This feature of stratified sampling has a direct impact on the efficiency of the overall calculation especially for cases where function evaluation is expensive. In the CCSS method, the variance of the sample mean was further reduced by introducing control-variate in the stratified sampling scheme. The control-variate in this approach plays an identical role as the importance function in Metropolis sampling. In this work, we have derived two different control-variates that are appropriate for MO integrals. The composite aspect of the CCSS method allows for evaluation of multiple MO integrals for the same stratified sampling step. Because the CCSS is a numerical method, it can be readily applied to complex kernels whose analytical integral in AO basis is not known. The developed CCSS method was applied for calculation of electron-hole matrix elements in the electron-hole explicitly correlated Hartree-Fock calculations and in the calculation of geminal-screened electron-hole interaction kernel. These methods were applied for investigation of excitonic properties of quantum dots. In both cases, the CCSS method not only allowed us to avoid the expensive AO-to-MO transformations but also allowed us to avoid calculation of AO integrals with R12 terms.

We believe that the CCSS method will be relevant for large-scale quantum mechanical calculations where AO-to-MO transformation is prohibitively expensive, calculations that are integral-direct where the AO integrals not pre-computed and stored, real-space and grid-based methods, many-body theories that use complex explicitly-correlated 2-electron, 3-electron, and higher n-electron operators for treating electron-electron correlation, and excited state calculations (such as CIS, Tamm-Dancoff, Bethe-Salpeter, GSIK and others) that require a small subset of MO integrals.

V. ACKNOWLEDGMENTS

We are grateful to National Science Foundation (CHE-1349892) and Syracuse University for the financial support.

Appendix A: Expectation value and variance

We define a set of values X ,

$$X = \{x_1, x_2, \dots, x_N\}. \quad (\text{A1})$$

The expectation value on set X is defined by the following operation,

$$\mathbb{E}[X] = \frac{1}{N} \sum_i^N x_i. \quad (\text{A2})$$

We also define the following common notations,

$$aX \equiv \{ax_1, ax_2, \dots, ax_N\} \quad (\text{A3})$$

$$X + Y \equiv \{x_1 + y_1, x_2 + y_2, \dots, x_N + y_N\} \quad (\text{A4})$$

$$XY \equiv \{x_1y_1, x_2y_2, \dots, x_Ny_N\}. \quad (\text{A5})$$

Using this we can now write the following properties of \mathbb{E} ,

$$\mathbb{E}[aX] = a\mathbb{E}[X] \quad (\text{A6})$$

$$\mathbb{E}[X + Y] = \mathbb{E}[X] + \mathbb{E}[Y]. \quad (\text{A7})$$

These two properties can be combined into a single relationship,

$$\mathbb{E}\left[\sum_{\alpha}^M a_{\alpha}X_{\alpha}\right] = \sum_{\alpha}^M a_{\alpha}\mathbb{E}[X_{\alpha}]. \quad (\text{A8})$$

The variance is defined as,

$$\mathbb{V}[X] = \mathbb{E}[X^2] - \mathbb{E}[X]^2. \quad (\text{A9})$$

Analogously, the covariance is defined as,

$$\mathbb{C}[X, Y] = \mathbb{E}[XY] - \mathbb{E}[X]\mathbb{E}[Y]. \quad (\text{A10})$$

The variance has the following scaling property,

$$\mathbb{V}[aX] = a^2\mathbb{V}[X]. \quad (\text{A11})$$

Proof.

$$\mathbb{V}[aX] = \mathbb{E}[a^2X^2] - \mathbb{E}[aX]^2 \quad (\text{A12})$$

$$= a^2\mathbb{E}[X^2] - a^2\mathbb{E}[X]^2 \quad (\text{A13})$$

$$= a^2(\mathbb{E}[X^2] - \mathbb{E}[X]^2) \quad (\text{A14})$$

$$= a^2\mathbb{V}[X] \quad (\text{A15})$$

■

The variance of sum of distributions is given by the following equation,

$$\mathbb{V}\left[\sum_{\alpha}^M a_{\alpha}X_{\alpha}\right] = \sum_{\alpha\beta}^M a_{\alpha}a_{\beta}\mathbb{C}[X_{\alpha}, X_{\beta}]. \quad (\text{A16})$$

Proof.

$$\mathbb{V}\left[\sum_{\alpha}^M a_{\alpha}X_{\alpha}\right] = \mathbb{E}\left[\sum_{\alpha\beta}^M a_{\alpha}a_{\beta}X_{\alpha}X_{\beta}\right] - \mathbb{E}\left[\sum_{\alpha}^M a_{\alpha}X_{\alpha}\right]^2 \quad (\text{A17})$$

$$= \sum_{\alpha\beta}^M a_\alpha a_\beta \mathbb{E}[X_\alpha X_\beta] - \sum_{\alpha\beta}^M a_\alpha a_\beta \mathbb{E}[X_\alpha] \mathbb{E}[X_\beta] \quad (\text{A18})$$

$$= \sum_{\alpha\beta}^M a_\alpha a_\beta \mathbb{C}[X_\alpha, X_\beta] \quad (\text{A19})$$

■

In case X_α and X_β are uncorrelated then the covariance is zero,

$$\mathbb{C}[X_\alpha, X_\beta] = 0 \quad (\text{for } \alpha \neq \beta). \quad (\text{A20})$$

The above expression reduces to,

$$\mathbb{V}[\sum_{\alpha}^M a_\alpha X_\alpha] = \sum_{\alpha}^M a_\alpha^2 \mathbb{V}[X_\alpha] \quad (\text{for uncorrelated } X_\alpha). \quad (\text{A21})$$

The relationship between the variance in the sample mean and the variance of the underlying distribution can be obtained as follows,

$$\mathbb{V}[\mu] = \mathbb{V}[\frac{1}{N} \sum_i^N X_i] \quad (\text{A22})$$

Because all the samples are uncorrelated,

$$\mathbb{V}[\mu] = \frac{1}{N^2} \sum_i^N \mathbb{V}[X_i] \quad (\text{A23})$$

Since X_i is drawn from the same distributions, all instances of X_i have identical variance,

$$\mathbb{V}[\mu] = \frac{1}{N^2} (N \mathbb{V}[X]) \quad (\text{A24})$$

$$= \frac{\mathbb{V}[X]}{N} \quad (\text{A25})$$

- ¹B. Fales and B. Levine, "Nanoscale multireference quantum chemistry: Full configuration interaction on graphical processing units," *Journal of Chemical Theory and Computation* **11**, 4708–4716 (2015).
- ²J. W. Snyder Jr., B. S. Fales, E. G. Hohenstein, B. G. Levine, and T. J. Martinez, "A direct-compatible formulation of the coupled perturbed complete active space self-consistent field equations on graphical processing units," *The Journal of Chemical Physics* **146**, 174113 (2017).
- ³M. Katouda, A. Naruse, Y. Hirano, and T. Nakajima, "Massively parallel algorithm and implementation of ri-mp2 energy calculation for peta-scale many-core supercomputers," *Journal of Computational Chemistry*, 2623–2633 (2016).
- ⁴Y.-Y. Ohnishi, K. Ishimura, and S. Ten-no, "Massively parallel mp2-f12 calculations on the k computer," *International Journal of Quantum Chemistry* **115**, 333–341 (2015).
- ⁵B. Peng and K. Kowalski, "Highly efficient and scalable compound decomposition of two-electron integral tensor and its application in coupled cluster calculations," *Journal of Chemical Theory and Computation* **13**, 4179–4192 (2017).
- ⁶P. E. M. Lopes, "Fast calculation of two-electron-repulsion integrals: a numerical approach," *Theoretical Chemistry Accounts* **136**, 112 (2017).
- ⁷M. Piccardo and A. Soncini, "A full-pivoting algorithm for the cholesky decomposition of two-electron repulsion and spin-orbit coupling integrals," *Journal of Computational Chemistry* **38**, 2775–2783 (2017).
- ⁸L. N. Wirz, S. S. Reine, and T. B. Pedersen, "On resolution-of-the-identity electron repulsion integral approximations and variational stability," *Journal of Chemical Theory and Computation* **13**, 4897–4906 (2017).
- ⁹J. Boström, F. Aquilante, T. B. Pedersen, and R. Lindh, "Ab initio density fitting: Accuracy assessment of auxiliary basis sets from cholesky decompositions," *Journal of Chemical Theory and Computation* **5**, 1545–1553 (2009).
- ¹⁰B. I. Dunlap, J. W. D. Connolly, and J. R. Sabin, "On some approximations in applications of x theory," *The Journal of Chemical Physics* **71**, 3396–3402 (1979).
- ¹¹J. L. Whitten, "Coulombic potential energy integrals and approximations," *The Journal of Chemical Physics* **58**, 4496–4501 (1973).
- ¹²A. P. Rendell and T. J. Lee, "Coupled-cluster theory employing approximate integrals: An approach to avoid the input/output and storage bottlenecks," *The Journal of Chemical Physics* **101**, 400–408 (1994).
- ¹³A. Sodt, J. E. Subotnik, and M. Head-Gordon, "Linear scaling density fitting," *The Journal of Chemical Physics* **125**, 194109 (2006).
- ¹⁴H.-J. Werner, F. R. Manby, and P. J. Knowles, "Fast linear scaling second-order mller-pleeset perturbation theory (mp2) using local and density fitting approximations," *The Journal of Chemical Physics* **118**, 8149–8160 (2003).
- ¹⁵M. Feyereisen, G. Fitzgerald, and A. Komornicki, "Use of approximate integrals in ab initio theory. an application in mp2 energy calculations," *Chemical Physics Letters* **208**, 359 – 363 (1993).
- ¹⁶O. Vahtras, J. Almlf, and M. Feyereisen, "Integral approximations for lcao-scf calculations," *Chemical Physics Letters* **213**, 514 – 518 (1993).
- ¹⁷F. Weigend, "A fully direct ri-hf algorithm: Implementation, optimised auxiliary basis sets, demonstration of accuracy and efficiency," *Phys. Chem. Chem. Phys.* **4**, 4285–4291 (2002).
- ¹⁸T. Y. Takeshita, W. A. de Jong, D. Neuhauser, R. Baer, and E. Rabani, "Stochastic formulation of the resolution of identity: Application to second order mller-pleeset perturbation theory," *Journal of Chemical Theory and Computation* **13**, 4605–4610 (2017).
- ¹⁹I. Reggen and T. Johansen, "Cholesky decomposition of the two-electron integral matrix in electronic structure calculations," *The Journal of Chemical Physics* **128**, 194107 (2008).
- ²⁰F. Aquilante, T. B. Pedersen, and R. Lindh, "Low-cost evaluation of the exchange fock matrix from cholesky and density fitting representations of the electron repulsion integrals," *The Journal of Chemical Physics* **126**, 194106 (2007).
- ²¹N. H. F. Beebe and J. Linderberg, "Simplifications in the generation and transformation of two-electron integrals in molecular calculations," *International Journal of Quantum Chemistry* **12**, 683–705 (1977).
- ²²H. Koch, A. S. de Mers, and T. B. Pedersen, "Reduced scaling in electronic structure calculations using cholesky decompositions," *The Journal of Chemical Physics* **118**, 9481–9484 (2003).
- ²³I. Reggen and E. Wislff-Nilssen, "On the beebelinderberg two-electron integral approximation," *Chemical Physics Letters* **132**, 154 – 160 (1986).
- ²⁴C. Song and T. J. Martinez, "Analytical gradients for tensor hyper-contracted mp2 and sos-mp2 on graphical processing units," *The Journal of Chemical Physics* **147**, 161723 (2017).
- ²⁵C. Song and T. J. Martinez, "Atomic orbital-based sos-mp2 with tensor hypercontraction. ii. local tensor hypercontraction," *The Journal of Chemical Physics* **146**, 034104 (2017).
- ²⁶C. Song and T. J. Martinez, "Atomic orbital-based sos-mp2 with tensor hypercontraction. i. gpu-based tensor construction and exploiting sparsity," *The Journal of Chemical Physics* **144**, 174111 (2016).
- ²⁷E. G. Hohenstein, R. M. Parrish, and T. J. Martinez, "Tensor hypercontraction density fitting. i. quartic scaling second- and third-order mller-pleeset perturbation theory," *The Journal of Chemical Physics* **137**, 044103 (2012).
- ²⁸R. M. Parrish, E. G. Hohenstein, T. J. Martinez, and C. D. Sherrill, "Tensor hypercontraction. ii. least-squares renormalization," *The Journal of Chemical Physics* **137**, 224106 (2012).
- ²⁹R. M. Parrish, E. G. Hohenstein, T. J. Martinez, and C. D. Sherrill, "Tensor hypercontraction. ii. least-squares renormalization," *The Journal of Chemical Physics* **137**, 224106 (2012).
- ³⁰E. G. Hohenstein, R. M. Parrish, C. D. Sherrill, and T. J. Martinez, "Communication: Tensor hypercontraction. iii. least-squares tensor hypercontraction for the determination of correlated wavefunctions," *The Journal of Chemical Physics* **137**, 221101 (2012).
- ³¹E. G. Hohenstein, S. I. L. Kokkila, R. M. Parrish, and T. J. Martinez, "Quartic scaling second-order approximate coupled cluster singles and doubles via tensor hypercontraction: Thc-cc2," *The Journal of Chemical Physics* **138**, 124111 (2013).
- ³²R. M. Parrish, E. G. Hohenstein, T. J. Martinez, and C. D. Sherrill, "Discrete variable representation in electronic structure theory: Quadrature grids for least-squares tensor hypercontraction," *The Journal of Chemical Physics* **138**, 194107 (2013).
- ³³R. M. Parrish, E. G. Hohenstein, N. F. Schunck, C. D. Sherrill, and T. J. Martínez, "Exact tensor hypercontraction: A universal technique for the resolution of matrix elements of local finite-range n -body potentials in many-body quantum problems," *Phys. Rev. Lett.* **111**, 132505 (2013).
- ³⁴E. G. Hohenstein, S. I. L. Kokkila, R. M. Parrish, and T. J. Martinez, "Tensor hypercontraction equation-of-motion second-order approximate coupled cluster: Electronic excitation energies in o(n4) time," *The Journal of Physical Chemistry B* **117**, 12972–12978 (2013).
- ³⁵R. M. Parrish, C. D. Sherrill, E. G. Hohenstein, S. I. L. Kokkila, and T. J. Martinez, "Communication: Acceleration of coupled cluster singles and doubles via orbital-weighted least-squares tensor hypercontraction," *The Journal of Chemical Physics* **140**, 181102 (2014).
- ³⁶S. I. L. Kokkila Schumacher, E. G. Hohenstein, R. M. Parrish, L.-P. Wang, and T. J. Martinez, "Tensor hypercontraction second-order mller-pleeset perturbation theory: Grid optimization and reaction energies," *Journal of Chemical Theory and Computation* **11**, 3042–3052 (2015).
- ³⁷W. Klopper, F. R. Manby, S. Ten-No, and E. F. Valeev, "R12 methods in explicitly correlated molecular electronic structure theory," *International Reviews in Physical Chemistry* **25**, 427–468 (2006).

- ³⁸S. A. Varganov and T. J. Martinez, "Variational geminal-augmented multireference self-consistent field theory: Two-electron systems," *The Journal of Chemical Physics* **132**, 054103 (2010).
- ³⁹B. A. Cagg and V. A. Rassolov, "Sspg: A strongly orthogonal geminal method with relaxed strong orthogonality," *The Journal of Chemical Physics* **141**, 164112 (2014), 10.1063/1.489925.
- ⁴⁰P. Jeszenszki, V. Rassolov, P. R. Surján, and Á. Szabados, "Local spin from strongly orthogonal geminal wavefunctions," *Molecular Physics* **113**, 249–259 (2015).
- ⁴¹V. Rassolov, "An ab initio linear electron correlation functional," *Journal of Chemical Physics* **110**, 3672–3677 (1999).
- ⁴²V. Rassolov, "Semiclassical electron correlation operator," *Journal of Chemical Physics* **131**, 204102 (2009).
- ⁴³V. Rassolov, "Harmonic electron correlation operator," *Journal of Chemical Physics* **135**, 034111 (2011).
- ⁴⁴B. Nichols and V. A. Rassolov, "Description of electronic excited states using electron correlation operator," *The Journal of Chemical Physics* **139**, 104111 (2013), 10.1063/1.482043.
- ⁴⁵S. A. Varganov and T. J. Martínez, "Variational geminal-augmented multireference self-consistent field theory: Two-electron systems," *The Journal of Chemical Physics* **132**, 054103 (2010), 10.1063/1.330326.
- ⁴⁶A. Grneis, S. Hirata, Y. ya Ohnishi, and S. Ten-no, "Perspective: Explicitly correlated electronic structure theory for complex systems," *The Journal of Chemical Physics* **146**, 080901 (2017).
- ⁴⁷S. Hirata, X. He, M. R. Hermes, and S. Y. Willow, "Second-order many-body perturbation theory: An eternal frontier," *The Journal of Physical Chemistry A* **118**, 655–672 (2014).
- ⁴⁸S. Hirata, M. R. Hermes, J. Simons, and J. V. Ortiz, "General-order many-body greens function method," *Journal of Chemical Theory and Computation* **11**, 1595–1606 (2015).
- ⁴⁹C. M. Johnson, A. E. Doran, J. Zhang, E. F. Valeev, and S. Hirata, "Monte carlo explicitly correlated second-order many-body perturbation theory," *The Journal of Chemical Physics* **145**, 154115 (2016).
- ⁵⁰S. Y. Willow, K. S. Kim, and S. Hirata, "Brueckner-goldstone quantum monte carlo for correlation energies and quasiparticle energy bands of one-dimensional solids," *Phys. Rev. B* **90**, 201110 (2014).
- ⁵¹S. Y. Willow, J. Zhang, E. F. Valeev, and S. Hirata, "Communication: Stochastic evaluation of explicitly correlated second-order many-body perturbation energy," *The Journal of Chemical Physics* **140**, 031101 (2014).
- ⁵²Y. Yang, K. R. Brorsen, T. Culpitt, M. V. Pak, and S. Hammes-Schiffer, "Development of a practical multicomponent density functional for electron-proton correlation to produce accurate proton densities," *The Journal of Chemical Physics* **147**, 114113 (2017).
- ⁵³A. K. Harshan, T. Yu, A. V. Soudackov, and S. Hammes-Schiffer, "Dependence of vibronic coupling on molecular geometry and environment: Bridging hydrogen atom transfer and electronproton transfer," *Journal of the American Chemical Society* **137**, 13545–13555 (2015).
- ⁵⁴A. Sirjoosingh, M. V. Pak, K. R. Brorsen, and S. Hammes-Schiffer, "Quantum treatment of protons with the reduced explicitly correlated hartree-fock approach," *The Journal of Chemical Physics* **142**, 214107 (2015).
- ⁵⁵A. Sirjoosingh, M. V. Pak, and S. Hammes-Schiffer, "Multicomponent density functional theory study of the interplay between electron-electron and electron-proton correlation," *The Journal of Chemical Physics* **136**, 174114 (2012).
- ⁵⁶A. Sirjoosingh and S. Hammes-Schiffer, "Diabatization schemes for generating charge-localized electronproton vibronic states in proton-coupled electron transfer systems," *Journal of Chemical Theory and Computation* **7**, 2831–2841 (2011).
- ⁵⁷A. Sirjoosingh, M. V. Pak, and S. Hammes-Schiffer, "Derivation of an electronproton correlation functional for multicomponent density functional theory within the nuclearelectronic orbital approach," *Journal of Chemical Theory and Computation* **7**, 2689–2693 (2011).
- ⁵⁸C. Ko, M. V. Pak, C. Swalina, and S. Hammes-Schiffer, "Alternative wavefunction ansatz for including explicit electron-proton correlation in the nuclear-electronic orbital approach," *The Journal of Chemical Physics* **135**, 054106 (2011).
- ⁵⁹A. Chakraborty and S. Hammes-Schiffer, "Density matrix formulation of the nuclear-electronic orbital approach with explicit electron-proton correlation," *The Journal of Chemical Physics* **129**, 204101 (2008).
- ⁶⁰A. Chakraborty, M. V. Pak, and S. Hammes-Schiffer, "Development of electron-proton density functionals for multicomponent density functional theory," *Phys. Rev. Lett.* **101**, 153001 (2008).
- ⁶¹A. Chakraborty, M. V. Pak, and S. Hammes-Schiffer, "Inclusion of explicit electron-proton correlation in the nuclear-electronic orbital approach using gaussian-type geminal functions," *The Journal of Chemical Physics* **129**, 014101 (2008).
- ⁶²C. Swalina, M. V. Pak, A. Chakraborty, and S. Hammes-Schiffer, "Explicit dynamical electronproton correlation in the nuclearelectronic orbital framework," *The Journal of Physical Chemistry A* **110**, 9983–9987 (2006).
- ⁶³C. Swalina, M. V. Pak, and S. Hammes-Schiffer, "Alternative formulation of many-body perturbation theory for electronproton correlation," *Chemical Physics Letters* **404**, 394 – 399 (2005).
- ⁶⁴M. V. Pak and S. Hammes-Schiffer, "Electron-proton correlation for hydrogen tunneling systems," *Phys. Rev. Lett.* **92**, 103002 (2004).
- ⁶⁵J. M. Elward, B. Thallinger, and A. Chakraborty, "Calculation of electron-hole recombination probability using explicitly correlated hartree-fock method," *The Journal of Chemical Physics* **136**, 124105 (2012).
- ⁶⁶J. M. Elward and A. Chakraborty, "Effect of dot size on exciton binding energy and electronhole recombination probability in cdse quantum dots," *Journal of Chemical Theory and Computation* **9**, 4351–4359 (2013).
- ⁶⁷J. A. Scher, J. M. Elward, and A. Chakraborty, "Shape matters: Effect of 1d, 2d, and 3d isovolumetric quantum confinement in semiconductor nanoparticles," *The Journal of Physical Chemistry C* **120**, 24999–25009 (2016).
- ⁶⁸B. H. Ellis, S. Aggarwal, and A. Chakraborty, "Development of the multicomponent coupled-cluster theory for investigation of multiexcitonic interactions," *Journal of Chemical Theory and Computation* **12**, 188–200 (2016).
- ⁶⁹M. G. Bayne, Y. Uchida, J. Eller, C. Daniels, and A. Chakraborty, "Construction of explicitly correlated geminal-projected particle-hole creation operators for many-electron systems using the diagrammatic factorization approach," *Phys. Rev. A* **94**, 052504 (2016).
- ⁷⁰J. M. Elward and A. Chakraborty, "Effect of heterojunction on exciton binding energy and electronhole recombination probability in cdse/zns quantum dots," *Journal of Chemical Theory and Computation* **11**, 462–471 (2015).
- ⁷¹M. G. Bayne, J. Drogo, and A. Chakraborty, "Infinite-order diagrammatic summation approach to the explicitly correlated congruent transformed hamiltonian," *Phys. Rev. A* **89**, 032515 (2014).
- ⁷²J. M. Elward, F. J. Irudayanathan, S. Nangia, and A. Chakraborty, "Optical signature of formation of protein corona in the firefly luciferase-cdse quantum dot complex," *Journal of Chemical Theory and Computation* **10**, 5224–5228 (2014).
- ⁷³C. J. Blanton, C. Brenon, and A. Chakraborty, "Development of polaron-transformed explicitly correlated full configuration interaction method for investigation of quantum-confined stark effect in gaas quantum dots," *The Journal of Chemical Physics* **138**, 054114 (2013).
- ⁷⁴J. M. Elward, J. Hoja, and A. Chakraborty, "Variational solution of the congruently transformed hamiltonian for many-electron systems using a full-configuration-interaction calculation," *Phys. Rev. A* **86**, 062504 (2012).
- ⁷⁵J. M. Elward, J. Hoffman, and A. Chakraborty, "Investigation of electronhole correlation using ex-

- licitly correlated configuration interaction method,” *Chemical Physics Letters* **535**, 182 – 186 (2012).
- ⁷⁶C. Filippi and C. Umrigar, “Multiconfiguration wave functions for quantum monte carlo calculations of first-row diatomic molecules,” *Journal of Chemical Physics* **105**, 213–226 (1996).
- ⁷⁷R. Guareschi and C. Filippi, “Ground- and excited-state geometry optimization of small organic molecules with quantum monte carlo,” *Journal of Chemical Theory and Computation* **9**, 5513–5525 (2013).
- ⁷⁸S. Moroni, S. Sacconi, and C. Filippi, “Practical schemes for accurate forces in quantum monte carlo,” *Journal of Chemical Theory and Computation* **10**, 4823–4829 (2014).
- ⁷⁹F. Schautz, F. Buda, and C. Filippi, “Excitations in photoactive molecules from quantum monte carlo,” *Journal of Chemical Physics* **121**, 5836–5844 (2004).
- ⁸⁰H. Zufikri, C. Amovilli, and C. Filippi, “Multiple-resonance local wave functions for accurate excited states in quantum monte carlo,” *Journal of Chemical Theory and Computation* **12**, 1157–1168 (2016).
- ⁸¹D. M. Ceperley and L. Mitas, “Quantum monte carlo methods in chemistry,” in *Advances in Chemical Physics* (John Wiley & Sons, Inc., 2007) pp. 1–38.
- ⁸²W. A. Lester, S. M. Rothstein, and S. Tanaka, *Recent advances in quantum Monte Carlo methods*, Vol. 92 (World Scientific, 2002).
- ⁸³M. Nightingale and C. Umrigar, *Quantum Monte Carlo Methods in Physics and Chemistry*, Nato Science Series C: (Springer Netherlands, 1998).
- ⁸⁴R. Rubinstein and D. Kroese, *Simulation and the Monte Carlo Method*, Wiley Series in Probability and Statistics (Wiley, 2016).
- ⁸⁵C. Pruneau, *Data Analysis Techniques for Physical Scientists* (Cambridge University Press, 2017).
- ⁸⁶D. Kroese, T. Taimre, and Z. Botev, *Handbook of Monte Carlo Methods*, Wiley Series in Probability and Statistics (Wiley, 2013).
- ⁸⁷G. Fishman, *Monte Carlo: Concepts, Algorithms, and Applications*, Springer Series in Operations Research and Financial Engineering (Springer New York, 2013).
- ⁸⁸M. Kalos and P. Whitlock, *Monte Carlo Methods*, Monte Carlo Methods (Wiley, 2008).
- ⁸⁹L.-W. Wang and A. Zunger, “Pseudopotential calculations of nanoscale cdse quantum dots,” *Phys. Rev. B* **53**, 9579–9582 (1996).
- ⁹⁰B. H. Ellis and A. Chakraborty, “Investigation of many-body correlation in biexcitonic systems using electronhole multicomponent coupled-cluster theory,” *The Journal of Physical Chemistry C* **121**, 1291–1298 (2017).
- ⁹¹S. N. Inamdar, P. P. Ingole, and S. K. Haram, “Determination of band structure parameters and the quasi-particle gap of cdse quantum dots by cyclic voltammetry,” *ChemPhysChem* **9**, 2574–2579 (2008).
- ⁹²J. Jasieniak, M. Califano, and S. E. Watkins, “Size-dependent valence and conduction band-edge energies of semiconductor nanocrystals,” *ACS Nano* **5**, 5888–5902 (2011).
- ⁹³R. W. Meulenbergh, J. R. Lee, A. Wolcott, J. Z. Zhang, L. J. Terminello, and T. van Buuren, “Determination of the exciton binding energy in cdse quantum dots,” *ACS Nano* **3**, 325–330 (2009).
- ⁹⁴C. Querner, P. Reiss, S. Sadki, M. Zagorska, and A. Pron, “Size and ligand effects on the electrochemical and spectroelectrochemical responses of cdse nanocrystals,” *Physical chemistry chemical physics : PCCP*, *Phys. Chem. Chem. Phys.* **7**, 3204–3209 (2005).